Nanoparticle-based autoantigen delivery to Treg-inducing liver sinusoidal endothelial cells enables control of autoimmunity in mice

Carambia, Antonella; Freund, Barbara; Schwinge, Dorothee; Bruns, Oliver T; Salmen, Sunhild C; Ittrich, Harald; Reimer, Rudolph; Heine, Markus; Huber, Samuel; Waurisch, Christian; Eychmüller, Alexander; Wraith, David C; Korn, Thomas; Nielsen, Peter; Weller, Horst; Schramm, Christoph; Lüth, Stefan; Lohse, Ansgar W; Heeren, Joerg; Herkel, Johannes

DOI:
10.1016/j.jhep.2015.01.006

Document Version
Publisher's PDF, also known as Version of record

Citation for published version (Harvard):
Carambia, A, Freund, B, Schwinge, D, Bruns, OT, Salmen, SC, Ittrich, H, Reimer, R, Heine, M, Huber, S, Waurisch, C, Eychmüller, A, Wraith, DC, Korn, T, Nielsen, P, Weller, H, Schramm, C, Lüth, S, Lohse, AW, Heeren, J & Herkel, J 2015, 'Nanoparticle-based autoantigen delivery to Treg-inducing liver sinusoidal endothelial cells enables control of autoimmunity in mice', *Journal of Hepatology*, vol. 62, no. 6, pp. 1349-1356. https://doi.org/10.1016/j.jhep.2015.01.006

Research Article

JOURNAL OF HEPATOLOGY

Nanoparticle-based autoantigen delivery to Treg-inducing liver sinusoidal endothelial cells enables control of autoimmunity in mice

Antonella Carambia[1], Barbara Freund[2], Dorothee Schwinge[1], Oliver T. Bruns[3,†], Sunhild C. Salmen[4], Harald Ittrich[5], Rudolph Reimer[3], Markus Heine[2], Samuel Huber[1], Christian Waurisch[6], Alexander Eychmüller[6], David C. Wraith[7], Thomas Korn[8], Peter Nielsen[2], Horst Weller[4], Christoph Schramm[1], Stefan Lüth[1], Ansgar W. Lohse[1], Joerg Heeren[2], Johannes Herkel[1,*]

[1]*Department of Medicine I, University Medical Center Hamburg-Eppendorf, Hamburg, Germany;* [2]*Department of Biochemistry and Molecular Cell Biology, University Medical Center Hamburg-Eppendorf, Hamburg, Germany;* [3]*Department of Electron Microscopy and Micro Technology, Heinrich-Pette Institute, Hamburg, Germany;* [4]*Institute of Physical Chemistry, University of Hamburg, Hamburg, Germany;* [5]*Department of Diagnostic and Interventional Radiology, University Medical Center Hamburg-Eppendorf, Hamburg, Germany;* [6]*Physical Chemistry, TU Dresden, Dresden, Germany;* [7]*Cellular and Molecular Medicine, University of Bristol, Bristol, UK;* [8]*Department of Neurology, TU München, München, Germany*

Background & Aims: It is well-known that the liver can induce immune tolerance, yet this knowledge could, thus far, not be translated into effective treatments for autoimmune diseases. We have previously shown that liver sinusoidal endothelial cells (LSECs) could substantially contribute to hepatic tolerance through their ability to induce CD4+ Foxp3+ regulatory T cells (Tregs). Here, we explored whether the Treg-inducing potential of LSECs could be harnessed for the treatment of autoimmune disease.

Methods: We engineered a polymeric nanoparticle (NP) carrier for the selective delivery of autoantigen peptides to LSECs *in vivo*. In the well-characterized autoimmune disease model of experimental autoimmune encephalomyelitis (EAE), we investigated whether administration of LSEC-targeting autoantigen peptide-loaded NPs could protect mice from autoimmune disease.

Results: We demonstrate that NP-based autoantigen delivery to LSECs could completely and permanently prevent the onset of clinical EAE. More importantly, in a therapeutic approach, mice with already established EAE improved rapidly and substantially following administration of a single dose of autoantigen peptide-loaded NPs, whereas the control group deteriorated. Treatment efficacy seemed to depend on Tregs. The Treg frequencies in the spleens of mice treated with autoantigen peptide-loaded NPs were significantly higher than those in vehicle-treated mice. Moreover, NP-mediated disease control was abrogated after Treg depletion by repeated administration of Treg-depleting antibody.

Conclusion: Our findings provide proof of principle that the selective delivery of autoantigen peptides to LSECs by NPs can induce antigen-specific Tregs and enable effective treatment of autoimmune disease. These findings highlight the importance of Treg induction by LSECs for immune tolerance.

Keywords: LSECs; Hepatic tolerance; Autoimmunity; Regulatory T cells; Nanomedicine.

Received 4 August 2014; received in revised form 19 December 2014; accepted 5 January 2015; available online 21 January 2015

* Corresponding author. Address: Department of Medicine I, University Medical Center Hamburg-Eppendorf, Martinistr. 52, 20246 Hamburg, Germany. Tel.: +49 7410 59736; fax: +49 7410 58014.

E-mail address: jherkel@uke.de (J. Herke).

† Present address: Department of Chemistry, Massachusetts Institute of Technology, Cambridge, MA, United States.

Abbreviations: LSEC, liver sinusoidal endothelial cell; Treg, regulatory T cell; NP, nanoparticle; EAE, experimental autoimmune encephalomyelitis; MBP, myelin basic protein; MOG, myelin oligodendrocyte glycoprotein; MRI, magnetic resonance imaging; DC, dendritic cell.

Introduction

The liver is well-known for its ability to promote immune tolerance rather than inflammation. This capability is of importance to prevent inadequate inflammatory immune responses against harmless gut-derived bacterial or nutritional antigens that constantly reach the liver via the portal blood [1]. Various liver-resident antigen-presenting cells, including liver dendritic cells (DCs), Kupffer cells and liver sinusoidal endothelial cells (LSECs) are involved in the maintenance of hepatic tolerance [2]. Notably LSECs have a well-described capability to suppress pro-inflammatory activities of CD4+ and CD8+ T cells [3–5]. Hepatic tolerance can be relevant for the control of inflammatory immune responses even outside of the liver, as indicated by the finding that hepatic expression of a myelin antigen facilitated protection from autoimmune neuroinflammation [6]. Notwithstanding the accumulated knowledge of the tolerance-inducing properties of the liver and LSECs in particular, efficient methods that could translate this knowledge into effective therapies for autoimmune diseases are still lacking.

Currently, causative treatments for autoimmune diseases are not established, and the available symptomatic treatments mainly rely on generalized immune suppression, producing systemic and often severe side effects, notably after long-term treatment [7,8]. In an attempt to develop more specific treatments of autoimmune diseases, therapies based on CD4+ Foxp3+ regulatory T cells (Tregs), which have a profound ability to control immune responses [9], are being explored. Tregs are also being considered for treatment of autoimmune liver inflammation [10–12]. However, a major obstacle to the clinical application of Tregs for therapy is the lack of efficient techniques for inducing antigen-specific Tregs *in vivo* [8,13]. We reasoned that this obstacle could be overcome by harnessing LSECs for antigen-specific Treg induction, as we had recently demonstrated that LSECs are efficient inducers of CD4+ Foxp3+ Tregs [14]. Therefore, we explored whether nanoparticle (NP)-based delivery of autoantigen peptides to Treg-inducing LSECs might serve the specific treatment of autoimmune disease.

Many types of NPs are known to accumulate in the liver shortly after administration *in vivo* [15], most of which are actively taken up by Kupffer cells. These liver-resident macrophages are major scavenger cells that phagocytose preferentially larger particles [16]. LSECs are a second type of scavenger cell in the liver that endocytose preferentially soluble macromolecules and small particles [16]. We reasoned that the differential scavenger preference of these liver cells could allow for the development of an NP carrier that might facilitate selective delivery of autoantigen peptides to LSECs *in vivo*.

We show that a small polymer-coated NP can facilitate rapid and selective delivery of autoantigen peptides to LSECs *in vivo*. In the well-established and clinically relevant mouse model of multiple sclerosis, experimental autoimmune encephalomyelitis (EAE) [17], which is marked by ascending paralysis, only a single administration of such LSEC-targeting NPs loaded with autoantigen peptides provided potent disease protection and therapy of established disease. Therefore, targeted delivery of autoantigen peptides to Treg-inducing LSECs by NPs represents a novel approach for the antigen-specific treatment of autoimmune diseases. Moreover, these findings demonstrate that LSECs seem to be major inducers of peripherally derived Tregs, and emphasize the importance of LSECs for maintaining immune tolerance.

Material and methods

Mice

B10.PL mice, tg4 mice [18], C57BL/6 mice, FVB mice, Foxp3gfp.KI mice [19] and hCD2-ΔkTβRII mice [20] were bred and kept in the animal facility of the University Medical Centre Hamburg-Eppendorf under specific pathogen-free conditions. F1 mice were generated by mating of Foxp3gfp.KI mice with tg4 mice. Mice were 6–12 weeks old at the start of experiments. Animal experiments were conducted in accordance with institutional guidelines and approved by the review board of the State of Hamburg, Germany.

Antibodies

For cell isolation and flow cytometry, fluorochrome-labelled antibodies were purchased from Miltenyi (Germany) (CD146), eBioscience (Germany) (Foxp3), BD Biosciences (Germany) (Syndecan-4) or Biolegend (Germany) (CD4, CD25, CXCR4).

Cell isolation and in vitro Treg conversion assay

Non-parenchymal liver cells were isolated as described [4] and further separated by MACS into CD146+ LSECs according to the manufacturer's instructions (Miltenyi Biotec, Germany). Treg conversion assays were performed with modifications as described [21]. CD4+CD25−Foxp3− T cells from (tg4 × Foxp3gfp.KI) F1 mice were sorted with a FACSaria (BD Biosciences, Germany). Treg conversion assays were performed in serum-free Panserin medium (Pan Biotech, Germany) by co-culture of non-Tregs (5×10^5/well) with LSECs, which had been pre-cultured for 24 h in collagen treated 96-well cell culture plates (1×10^5/well) in IMDM/10% FCS (Life technologies, PAA, Germany), in the presence of 2 ng/ml recombinant human TGF-β1 (R&D Systems, Germany). Myelin basic protein (MBP) peptide (Ac-ASQYRPSQR-COOH; Panatecs, Germany) coupled to NPs (MBP-NP) or, as controls, NPs without peptide load or free MBP peptide were used for T cell stimulation by LSECs. At day four of culture, T cells were stained for Foxp3 (Foxp3 Staining Buffer Set; eBioscience, Germany) and analysed with a LSRII cytometer (BD Bioscience, Germany).

Experimental autoimmune encephalomyelitis

200 μg MBP peptide (Panatecs, Germany) in PBS was emulsified with complete Freund's adjuvant containing 4 mg/ml heat-killed Mycobacterium tuberculosis, strain H37RA (Difco, USA) and administered subcutaneously to B10.PL mice as described [6]. As indicated, B10.PL mice were splenectomised seven days before EAE induction. C57BL/6 mice were inoculated subcutaneously with 100 μg emulsified myelin oligodendrocyte glycoprotein (MOG) peptide (MEVGWYRSPFSRVVHLYRNGK, Panatecs, Germany). Additionally, 200 ng pertussis toxin (Sigma-Aldrich, Germany) was injected intraperitoneally at the time of immunisation and 48 h later. EAE was monitored daily and clinical symptoms were scored as follows: 0, no detectable signs of EAE; 1, tail atony; 2, partial hind limb paralysis; 3, complete hind limb paralysis; 4, fore limb and hind limb paralysis; 5, moribund.

Preparation of polymer-coated peptide-coupled NPs

^{59}Fe-labelled [22] and unlabelled [23] superparamagnetic iron oxide nanocrystals or CdSe/CdS/ZnS-core-shell-shell quantum dots [24] were encapsulated into an amphiphilic polymer (poly(maleic anhydride-alt-1-octadecene)) as described [25]. Coupling of NPs (6 μmol/L) to peptides with 1-Ethyl-3-(3-dimethylaminopropyl)-carbodiimide (6 mmol/L) was conducted as described [26]. A 1000-fold (MBP) or 100-fold (MOG) excess of the peptide was added and incubated overnight. Free peptide was removed under centrifugal force in a filter device (10 times, 100 kDa, 2500 g, 4 °C).

Determination of peptide-nanoparticle coupling efficiency

Using different excesses of ^{14}C-labelled MBP peptide, the amount coupled to the NPs was calculated on basis of the initial amount used, the amount of ^{14}C-labelled peptides coupled to NPs pelleted by ultracentrifugation and the amount of free ^{14}C-labelled peptide in the filtrate, as determined by liquid scintillation counting.

Turnover studies and organ distribution of nanoparticles

Anaesthetized mice were intravenously injected with 200 μl of a solution of ^{59}Fe-labelled NPs coupled to unlabelled MBP peptide or unlabelled NPs coupled to ^{14}C-MBP peptide. Plasma clearance was determined from 10 μl (^{14}C) or all gained (^{59}Fe) plasma 2, 5, 15, and 30 min after injection. After 60 min, blood was removed by cardiac puncture, and, after perfusion with PBS containing 50 U/ml heparin, organs were solubilized in Solvable (PerkinElmer) (0.1 ml/10 mg organ) for the measurement of ^{14}C-radioactivity in scintillation fluid. Uptake was calculated as percentage of activity in all measured organs. ^{59}Fe-activity was measured using the large volume Hamburg whole body radioactivity counter [27].

Apoptosis assay

Terminal deoxynucleotidyl transferase–mediated dUTP nick end labelling (TUNEL) was performed with the *In Situ* Cell Death Detection Kit, TMR-Red (Roche) on formalin-fixed liver sections of C57Bl/6 mice seven days after intravenous injection of MOG-NPs or PBS; cells were counterstained with Hoechst 33258 nuclear dye (Invitrogen). As positive control DNAse I-treatment was used (Roche).

In vivo imaging studies

Magnetic resonance imaging (MRI) and electron microscopy was performed as described [28,29]. The MRI parameters are described in Supplementary Table 1. For electron microscopy, 60 min after intravenous injection of MBP-NPs or NPs, mice were perfused with 2% glutaraldehyde in PBS, washed and post-fixed for 30 min with 1% OsO4 in PBS. Intravital microscopy was performed as described [29] with a confocal microscope equipped with a resonant scanner (Nikon A1R).

Nanoparticle-based autoantigen peptide delivery to LSECs in EAE

One day after EAE induction by immunisation to MBP or MOG peptide (B10.PL or C57BL/6 background, respectively), MBP- or MOG-loaded NPs (equivalent of 7 μg peptide/mouse as assessed by radioactive binding assays) were administered into the tail vein. Control mice were treated with equivalent doses of unloaded NPs or uncoupled peptide or PBS. Alternatively, MOG peptide-immunised mice were injected with MOG-NPs or PBS at the time of disease manifestation (day 8–12 post immunisation).

Treg depletion in vivo

B10.PL mice, which were treated with MBP peptide-coupled NPs or PBS after EAE induction, were intraperitoneally injected with 500 μg depleting antibody to CD25 (clone PC61, BioXcell, USA) or isotype-matched control antibody twice per week starting from day two post EAE induction.

Statistics

Statistical significance of differences between two data sets was calculated by the Mann-Whitney test; for comparison of multiple groups, the one-way ANOVA test and Tukey's post test were performed. A p value of less than 0.05 was considered significant.

Results

To select a NP that is selectively taken up by LSECs, we performed preliminary experiments with several types of NPs with a fluorescent quantum dot core [24], testing their uptake into mouse liver cells after intravenous administration by intravital microscopy. We found that a small NP with a poly(maleic anhydride-*alt*-1-octadecene)-coat [25,30] seemed to accumulate selectively in liver sinusoidal endothelium (Supplementary Fig. 1A). To generate an effective antigen carrier system, we chose a simple one-step coupling strategy using a carbodiimide crosslinking approach [26] to attach an autoantigen peptide to the polymer-coated NP with a superparamagnetic iron oxide core [23]. As a prototypic autoantigen, we used the multiple sclerosis-associated antigen MBP [18]. Each NP was loaded maximally with 100 peptide molecules per NP as demonstrated by binding assays with ^{14}C-radiolabelled MBP peptide (Supplementary Fig. 1B). Peptide loading did not influence charge, size, and shape of NPs as determined by measurement of the Zeta potential, size exclusion chromatography and electron microscopy (Supplementary Fig. 1C–E).

To investigate whether MBP peptide-loading of the NPs is stable *in vivo* or whether the peptide is cleaved off, kinetic turnover studies with ^{14}C-radiolabelled MBP peptide-NP conjugates (^{14}C-MBP-NP) were performed in comparison with ^{59}Fe-radiolabelled NPs [22] conjugated to non-labelled MBP peptide (MBP-^{59}Fe-NP). Both radiolabels were rapidly cleared with similar kinetics (Fig. 1A), predominantly by the liver (Fig. 1B). Low amounts of radioactivity could be detected in spleen and kidney, whereas uptake into other organs was negligible. This finding was in line with our recently published exact quantification of

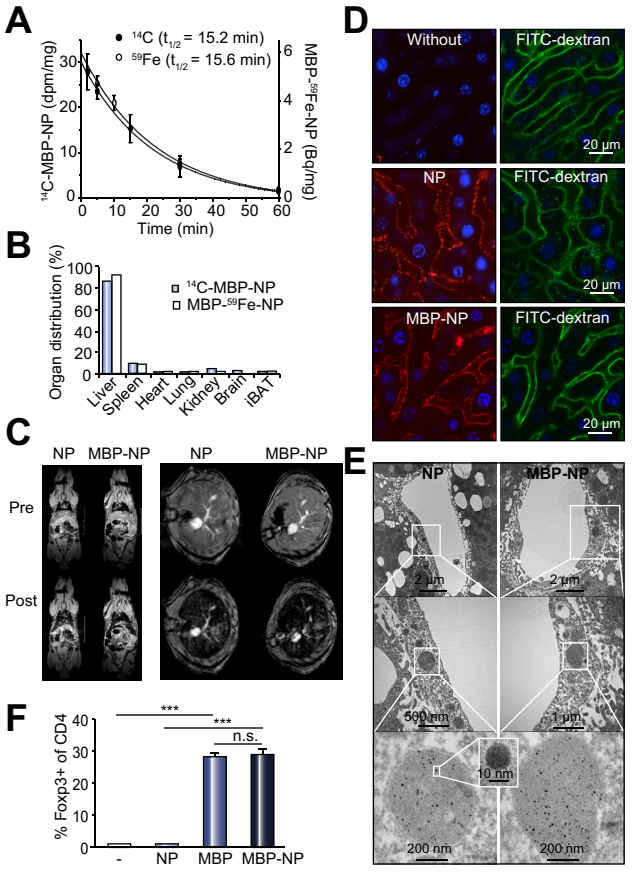

Fig. 1. Selective delivery of MBP peptide antigens to Treg-inducing LSECs *in vivo* by nanoparticles. (A) Plasma clearance rates of MBP peptide coupled to ^{59}Fe-NPs (MBP-^{59}Fe-NP) and ^{14}C-MBP peptide coupled to unlabelled NPs (^{14}C-MBP-NP). (B) Organ distribution of MBP-^{59}Fe-NPs and ^{14}C-MBP-NPs 60 min after intravenous injection into mice. Mean values ± SEM are shown. (C) Representative coronal (left) and transversal (right) MR images of mice before and after injection of unloaded NPs or MBP-NPs. (D) Intravital confocal microscopy of the liver showing uptake of MBP-NPs or unloaded NPs by LSECs. Blue, nuclei; green, LSECs (FITC-dextran); red, quantum dot-labelled NPs. Scale bar: 20 μm. (E) Electron microscopy of liver, 60 min after intravenous injection of MBP-NPs or unloaded NPs showing NP uptake into endosomal compartments of LSECs. (F) Splenic CD4+Foxp3− T cells from tg4 × Foxp3gfp.KI mice were co-cultured *in vitro* with LSECs in the presence of TGF-β (2 ng/ml) and free MBP peptide (5 ng/ml) or an equivalent dose of MBP peptide coupled to nanoparticles (MBP-NP) for four days; as controls, no peptide or empty NPs were added for T cell stimulation. Foxp3 induction in CD4+ T cells was then analysed by flow cytometry (unstimulated (−): 0.5 ± 0.004; empty NP: 0.5 ± 0; free MBP peptide: 28.3 ± 0.84; MBP-NP: 29.13 ± 1.751; p <0.0001).

organ distribution, using ^{51}Cr-radiolabelled NPs demonstrating that 91% of the injected radioactivity was taken up by the liver within 2 h [31]. In addition, we visualized organ uptake by dynamic MRI (Supplementary Table 1) [28], revealing hepatic targeting of both MBP peptide-loaded and unloaded NPs (Fig. 1C; Supplementary Movies 1 and 2). Thus, MBP peptides stay attached to the NPs *in vivo* and are not cleaved off and excreted via the kidney, but transported by the desired targeting effect of our NPs to liver cells.

To further investigate whether MBP peptide-loading altered the cellular tropism of administered peptide-NP conjugates, we performed conventional as well as intravital confocal fluorescence microscopy of the liver, using NPs with a fluorescent quantum dot core [29]. Prior to administration of fluorescent MBP

peptide-NP conjugates, recipient mice were injected with FITC-dextran which is rapidly absorbed by LSECs. After intravenous injection of MBP-NPs or unloaded NPs, we observed a rapid accumulation of both unloaded NPs and MBP-NPs in the liver, which clearly co-localized with FITC-dextran stained LSECs (Fig. 1D; Supplementary Movie 3). To further confirm uptake of peptide-loaded and unloaded NPs by LSECs, we performed transmission electron microscopy of liver slices, and detected considerable internalization of MBP peptide-NP conjugates into endosomal compartments of LSECs (Fig. 1E). Of note, uptake of NPs by LSECs did not induce apoptosis as assessed by TUNEL staining of liver slices seven days after *in vivo* administration of MBP-NPs (Supplementary Fig. 2). Together, these findings demonstrate that these NPs, with or without peptide cargo, are selectively taken up by LSECs, and thus facilitate efficient and selective delivery of autoantigen peptides to LSECs *in vivo*.

To assess whether LSECs can present NP-bound antigen peptides to T cells, thereby inducing antigen-specific Tregs, we studied Treg conversion of MBP-specific $CD4^{+}CD25^{-}Foxp3^{-}$ non-Tregs that were obtained from the spleens of (tg4 × Foxp3gfp.KI) F1 mice. These non-Treg cells are MBP-specific [18] and were sorted based on the absence of the Foxp3-linked expression of green fluorescent protein (GFP) [19]. The non-Treg cells were stimulated by LSECs *in vitro* in the presence of free MBP peptide or of MBP peptide bound to NPs (MBP-NPs) and exogenous active TGF-β, which is required for Treg conversion [20]. We found that LSEC-induced Treg generation occurred with similar efficacy in the presence of free MBP peptide or of NP-bound MBP peptide, but not of unloaded NPs (Fig. 1F), indicating that NP-bound MBP peptide antigen was presented by LSECs to facilitate Treg induction.

The proposed immunosuppressive effect of LSEC-targeting MBP-NPs *in vivo* was first tested in MBP-induced EAE in B10.PL mice (Fig. 2A). Intriguingly, a single intravenous injection of MBP–NPs one day after EAE induction provoked a lasting and complete protection from clinical EAE; in contrast, control mice treated with PBS or with unloaded NPs developed clinical EAE symptoms, including hind limb paralysis (Fig. 2A). Remarkably, even tg4 mice [18], which feature MBP-specific CD4+ T cells and develop more severe EAE than wild-type mice, were protected from disease by a single MBP-NP injection one day after EAE induction (Fig. 2B). Control mice receiving an equivalent dose of free MBP peptide, in contrast, developed severe EAE cumulating in complete paralysis of all four limbs (Fig. 2B). To confirm the treatment efficacy of NP-based autoantigen delivery to LSECs in another independent disease model, we tested the effect of NPs loaded with MOG peptides on the development of MOG-induced EAE in C57BL/6 mice. Consistent with our observations in MBP-induced EAE of B10.PL mice, administration of MOG–NPs to C57BL/6 mice one day after EAE induction completely protected recipient mice from developing any clinical disease symptom. In contrast, control mice receiving unloaded NPs developed EAE with hind limb paralysis (Fig. 2C).

Although we have shown in Fig. 1B that more than 90% of injected NPs accumulate in the liver, it was possible that the spleen, accumulating some 5% of the injected NPs, was responsible for NP-mediated tolerance. To address this issue, we performed splenectomy in B10.PL mice before EAE induction and treatment with MBP-NPs. Clearly, MBP-NPs induced disease protection in splenectomised mice, indicating that the spleen is dispensable for tolerance induction. However, MBP-NP induced

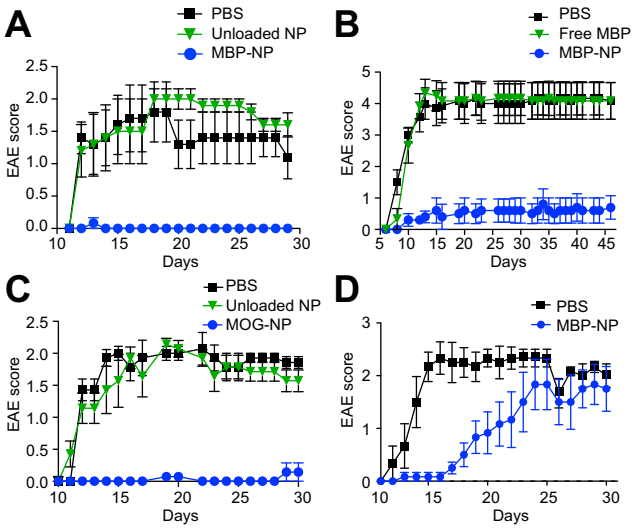

Fig. 2. Prevention of EAE by nanoparticle-based delivery of autoantigen peptides to LSECs. EAE was induced in B10.PL mice (A) or tg4 mice (B) by immunisation to MBP peptide. In C57BL/6 mice (C), EAE was induced by immunisation to MOG peptide. For disease prevention, mice were injected once intravenously with PBS (black squares), MBP-NPs (A, B, blue circles) or MOG-NPs (C, blue circles) one day after EAE induction. As treatment control, mice received equivalent amounts of unloaded NPs (A, C, green triangles) or unconjugated MBP peptide (B, green triangles). Splenectomy was performed in B10.PL mice and EAE was induced 7 days later by immunisation to MBP peptide. One day after EAE induction, mice were injected once intravenously with MBP-NPs (blue circles) or PBS (black squares) (D). Shown are mean EAE scores ± SEM. (n = 5–7). Group comparisons were performed with the Mann-Whitney test or with one-way ANOVA and Tukey's post test.

tolerance was gradually lost in splenectomised mice after day 16, indicating that the spleen is required for the maintenance of tolerance induced by the liver (Fig. 2D).

Having determined that LSEC-targeting autoantigen peptide-loaded NPs effectively prevented autoimmune disease development, we addressed the even more important issue of whether autoantigen peptide delivery to LSECs can serve as therapy of established autoimmune disease. Therefore, we first induced clinical EAE in C57BL/6 mice by MOG-immunisation. At the time of treatment, both the recipients of MOG-NPs and control mice showed clinical symptoms, such as a waggly gait, with similar disease scores (Fig. 3A). The control group progressed in EAE severity towards hind limb paralysis; in contrast, the mean clinical scores of MOG-NP treated mice improved rapidly and substantially towards a normal gait (Fig. 3B and C). Of note, disease control induced by a single therapeutic injection of MOG-NPs continued throughout an extended follow-up period of 9 weeks (Fig. 3B and C). Therefore, NP-mediated autoantigen delivery to LSECs seemed to provide robust and effective therapy of established autoimmune disease. To confirm that NP-mediated antigen delivery to LSECs induced the generation of Tregs *in vivo*, we treated MOG-immunised C57BL/6 mice with MOG-NPs or PBS and analysed the Treg frequencies in the spleen after seven days. We found that the Treg frequencies in the spleens of MOG-NP treated mice were significantly higher than those in PBS treated mice (Fig. 4A). As we have shown before that Treg induction by LSECs required TGF-β signaling to T cells [14], we reasoned that NP-based targeting of autoantigen peptides to LSECs should be ineffective in mice with TGF-β insensitive T cells. Indeed,

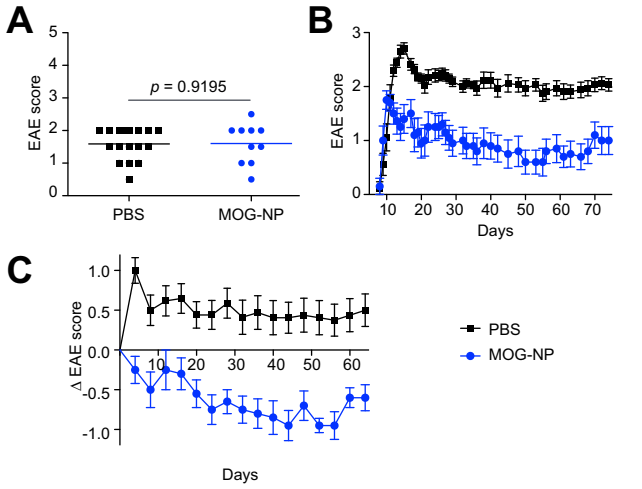

Fig. 3. Therapy of established EAE by nanoparticle-mediated delivery of autoantigen peptides to LSECs. EAE was induced in C57BL/6 mice by immunisation to MOG peptide. For therapy of established disease, mice were treated once after disease onset with a single injection of MOG-NPs (n = 10, blue circles) or PBS (n = 17, black squares). (A) Similar initial disease scores at the time of treatment in PBS treated or MOG-NP treated groups (mean score 1.59 ± 0.12 *vs.* 1.60 ± 0.19; $p = 0.9195$). (B) EAE course over an extended observational period of more than nine weeks after MOG-NP (blue) or PBS (black) treatment. (C) Mean score difference (ΔEAE score) compared to the time of treatment with MOG-NPs (blue) or PBS (black). Group comparisons were performed with the Mann-Whitney test.

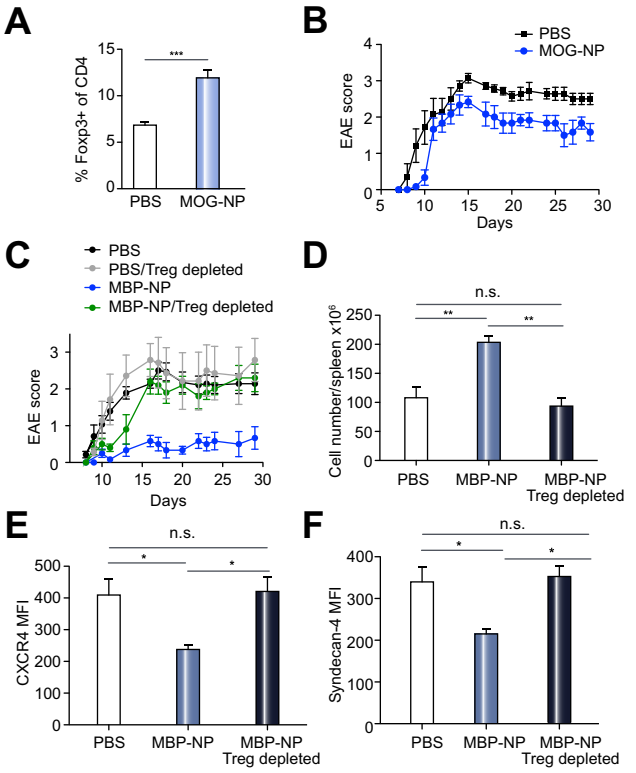

Fig. 4. Nanoparticle-based disease control by LSECs is Treg-dependent. (A) EAE was induced in C57BL/6 mice by MOG-immunisation, followed by PBS or MBP-NP treatment one day after EAE induction; induced Tregs in spleens were assessed seven days after EAE induction. (B) EAE was induced by immunisation to MOG peptide in hCD2-ΔkTβ RII mice bearing TGF-β insensitive T cells. One day after EAE induction, mice were injected once with PBS (black) or MOG-NPs (blue). (C) EAE was induced in B10.PL mice by immunisation to MBP peptide. One day after EAE induction, mice were injected once with PBS or MBP-NPs. In addition, mice received twice weekly a Treg-depleting antibody (green: MBP-NP/Treg-depleted; grey: PBS/Treg-depleted) or isotype-matched control antibody (blue: MBP-NP; black: PBS) (n = 5–7). (D–F) Mice were treated as described in (C) and absolute spleen cell numbers (D) as well as CXCR4 (E) and Syndecan-4 (F) expression were assessed. For statistical analysis, the Mann-Whitney test (A, B), or one-way ANOVA and Tukey's post test (C–F) were used. The mean EAE scores ± SEM are shown.

MOG–NPs induced only a minor degree of protection from EAE in hCD2-ΔkTβRII mice [20], which feature TGF-β insensitive T cells (Fig. 4B). Thus, we can conclude that the efficacy of NP-mediated disease protection was dependent on TGF-β signals to T cells, which are required for peripheral Treg induction. To directly test whether NP-mediated protection from EAE was dependent on Treg function *in vivo*, we depleted Tregs in mice that had received MBP-NPs by repeated administration of the Treg-depleting PC61 antibody [32] (Fig. 4C); the efficacy of depletion was confirmed by flow cytometry (Supplementary Fig. 3). Although administration of MBP-NPs induced protection from EAE in control mice, MBP-NPs could not prevent the development of disease in Treg-depleted mice (Fig. 4C). In fact, the disease severity precipitated by Treg depletion was similar to the disease severity of the control group receiving PBS instead of MBP-NP (Fig. 4C), demonstrating that Tregs are critically involved in NP-mediated control of autoimmune disease.

We observed that disease-resistant mice following MBP-NP treatment exhibited significantly increased cell numbers in the spleen, as compared to PBS treated mice with disease (Fig. 4D). Moreover, this increase in cell numbers seemed to depend on Tregs, as it was not observed in Treg-depleted mice following MBP-NP treatment (Fig. 4D). These findings indicate that functional Tregs in MBP-NP treated mice seemed to prevent the egress of effector cells from the spleen. The retention of effector cells in the spleen was recently published as an important suppressor mechanism by Tregs [33]. Since Treg-induced splenic retention seems to be associated with a downregulation of CXCR4 and Syndecan-4 on effector cells [33], we analysed the expression of these molecules in the spleens of MBP-NP treated mice. As compared to PBS treated control mice with manifest disease, splenocytes of MBP-NP treated disease-resistant mice exhibited significantly lower expression of CXCR4 (Fig. 4E) and Syndecan-4 (Fig. 4F). Treg depletion in MBP-NP treated mice resulted in expression levels of CXCR4 and Syndecan-4 that were as high as those in the PBS treated controls (Fig. 4E and F). Note that also the disease severity at the time of analysis of Treg-depleted mice following MBP-NP treatment (2.3 ± 0.4) was similar to that of the PBS treated control mice (2.2 ± 0.3), whereas Treg-replete MBP-NP treated mice did not exhibit severe EAE (0.6 ± 0.4).

Discussion

A major obstacle to a causative treatment for autoimmune diseases is the lack of efficient techniques to induce specific suppression of the autoreactive T cells that attack the host tissue. Treg-based therapies have the potential to provide the desired specific immune suppression, as autoantigen-specific Tregs have a profound ability to control immune responses to their cognate self-antigens [8,9]. However, these therapies are greatly limited by the insufficiency of techniques for inducing antigen-specific

Tregs *in vivo* [8,13]. Here we show that LSECs can be harnessed to effectively control the development and progression of autoimmune disease. By taking advantage of NPs that are selectively taken up by LSECs, we developed a tool for efficient and selective delivery of autoantigen peptides to Treg-inducing LSECs (Fig. 1). Intriguingly, a single administration of such LSEC-targeting NPs loaded with autoantigen peptides provided effective disease control (Figs. 2 and 3) that was mediated by Tregs (Fig. 4). Therefore, our findings might enable the development of causative treatments for autoimmune diseases that operate through the efficient induction of antigen-specific Tregs *in vivo*.

The poly(maleic anhydride-alt-1-octadecene)-coated NPs that we have used in the current study were selected based on their properties with regard to cellular distribution and processing, as well as their preferential accumulation in the liver [22]. These NPs accumulated to more than 90% in the liver within 2 h after injection (Fig. 1) [31]. As we could induce full disease protection with as little as 7 μg NP-bound peptide per mouse, we can thus deduce that 6.4 μg peptide was taken up by the liver, whereas only 0.3 μg peptide had been delivered to the spleen and even less to other organs. To exclude that the spleen, although accumulating only a minor peptide dose, was responsible for the induced disease control, we performed splenectomy before NP-treatment (Fig. 2D). Our finding that MBP-NPs induced disease protection also in splenectomised mice indicated that the spleen was dispensable for tolerance induction. As the peptide dose potentially delivered to lymph nodes was below 0.09 μg, we believe that the role of lymph nodes in NP-mediated disease control was negligible. Nonetheless, we cannot fully exclude a minor participation of non-hepatic cells in tolerance induction.

Although LSECs seem to accumulate the majority of the administered NPs, it was possible that NPs could be secondarily delivered to Kupffer cells, e.g. by phagocytosis of apoptotic LSECs after NP-induced cell death. We therefore assessed the vitality of LSECs after NP administration by TUNEL assay (Supplementary Fig. 2) and did not find any increase in apoptosis. Moreover, as assessed by electron microscopy, NP accumulation did not result in compromised cell integrity or cell death. Indeed, LSECs that had taken up NPs were detectable by iron accumulation in electron microscopy even four weeks after NP administration (not shown). Thus, it was unlikely that uptake of NPs by LSECs had induced significant cell death, and that Kupffer cells had secondarily accumulated NPs. Nonetheless, Kupffer cells, like LSECs, have the capability to induce Tregs [14]; thus, it is reasonable to assume that NP uptake by Kupffer cells could contribute to NP-induced tolerance.

The mechanisms that govern preferential NP uptake by LSECs remain to be determined, but one may speculate that the combination of a negative charge mediated by the polymer coat with relatively small particle size tags these NPs for uptake by LSECs, which are believed to be the major scavenger cell type for small particles [16]. Nanoparticles targeting splenic DCs [34] or macrophages [35] are also being explored as tools for antigen-specific tolerance induction. However both, DCs [36] and macrophages [37], display a high degree of plasticity and readily can differentiate to inflammatory cells [2], advocating co-delivery of suppressive immune mediators [34]. In contrast, LSECs display a robust immunosuppressive phenotype even in the presence of pro-inflammatory signals [2,38]. Indeed, LSECs are not only potent inducers of Tregs [14], but also potent suppressors of inflammatory CD4+ and CD8+ T cell effector responses [3–5,39,40]. Therefore, antigen delivery to LSECs may avoid the risk of disease exacerbation that remains when attempting to treat individuals with on-going inflammation by targeting autoantigen to DCs or macrophages. Indeed, the NP treated mice did not exhibit obvious signs of toxicity or adverse reactions, at least not within an observation period of up to nine weeks. An additional safety feature of the NPs used here is their iron oxide core that could allow MR-based monitoring of the biodistribution of NP peptide conjugates *in vivo* (Supplementary Movies 1 and 2), when therapeutically applied to patients.

CD4+Foxp3+ Tregs are not only generated in the thymus, but also in the periphery through TGF-β dependent conversion from conventional CD4+ T cells. Thymus-derived Tregs and peripherally derived Tregs have dissimilar T cell receptor repertoires [41], covering different antigen sets. Peripheral Treg generation is particularly relevant for maintaining tolerance to antigens that are not represented in the thymus. We found an increase in Tregs in the spleen of mice after treatment with peptide-loaded NPs (Fig. 4A). We also found a tendency towards a lower proportion of Nrp-1 expressing cells [41] in mice treated with peptide-loaded NPs (not shown), which might indicate a relative increase in peripherally induced Tregs in the NP treated animals. However, in-depth analysis of phenotype and function of NP-induced Tregs could not be performed with the necessary sensitivity, as it was not possible to separate NP-induced Tregs from the other endogenously induced Tregs. Thus, when resorting to analysis of the Tregs in bulk, we did not find significant differences in CD39 or CD73 expression or suppressive capacity between Tregs of NP treated or PBS treated mice (not shown). Nevertheless, the NP-induced increase in antigen-specific Tregs seemed to be instrumental in disease protection (Fig. 4).

Our findings highlight that LSECs are relevant inducers of peripherally derived Tregs. Note that LSECs can take up large amounts of circulating antigens [42]; therefore, LSECs may induce Tregs specific for both hepatic and non-hepatic antigens. As we show here, the potential of Treg induction by LSECs can be unleashed using an NP carrier for selective transport of peptides to LSECs. Indeed, our data provides proof of principle that autoimmune diseases can be effectively treated through NP-based antigen delivery to LSECs. Due to the versatility of peptide loading onto these NPs, this methodology might be applicable to a wide range of inflammatory diseases in which the driving antigens have been identified. We therefore believe that our findings enable the development of a clinically applicable treatment for various human diseases, including autoimmune diseases like multiple sclerosis and allergies.

Financial support

Supported by grants from the 'Deutsche Forschungsgemeinschaft' – Germany (SFB 841; SPP1313), from the 'Bundesministerium für Bildung und Forschung' – Germany (TOMCAT (01 EZ 0824), from the Hamburg State excellence initiative Nanotechnology in Medicine (NAME) – Germany, and from the 'Wellcome Trust' – United Kingdom (grant (090175/Z/09/Z).

Conflict of interest

The authors declare that there are no conflicts of interest to disclose.

Authors' contributions

A.C., B.F., J. Hee, and J. Her, designed the study and wrote the manuscript. A.C., B.F., D.S., O.T.B., S.C.S., H.I., R.R., M.H., J. Hee, and J. Her, performed and analysed experiments. O.T.B., S.H., P.N., H.W., C.S., S.L., and A.W.L. gave technical or conceptual advice. S.C.S., C.W., A.E., D.C.W., T.K., H.W., and C.S. provided essential material or mice.

Acknowledgments

We are grateful for excellent technical assistance by Sandra Ehret, Hendrik Herrmann, Marko Hilken, Agnes Malotta, and Christina Trabandt. Furthermore, we thank Michael G. Kaul for the development and implementation of the MR imaging sequences. Cell sorting was performed by the flow cytometry core facility of the University Medical Centre Hamburg-Eppendorf.

Supplementary data

Supplementary data associated with this article can be found, in the online version, at http://dx.doi.org/10.1016/j.jhep.2015.01.006.

References

[1] Racanelli V, Rehermann B. The liver as an immunological organ. Hepatology 2006;43:S54–S62.
[2] Thomson AW, Knolle PA. Antigen-presenting cell function in the tolerogenic liver environment. Nat Rev Immunol 2010;10:753–766.
[3] Knolle PA, Schmitt E, Jin S, Germann T, Duchmann R, Hegenbarth S, et al. Induction of cytokine production in naive CD4[+] T cells by antigen-presenting murine liver sinusoidal endothelial cells but failure to induce differentiation toward Th1 cells. Gastroenterology 1999;116:1428–1440.
[4] Carambia A, Frenzel C, Bruns OT, Schwinge D, Reimer R, Hohenberg H, et al. Inhibition of inflammatory CD4 T cell activity by murine liver sinusoidal endothelial cells. J Hepatol 2013;58:112–118.
[5] Limmer A, Ohl J, Kurts C, Ljunggren HG, Reiss Y, Groettrup M, et al. Efficient presentation of exogenous antigen by liver endothelial cells to CD8+ T cells results in antigen-specific T-cell tolerance. Nat Med 2000;6:1348–1354.
[6] Lüth S, Huber S, Schramm C, Buch T, Zander S, Stadelmann C, et al. Ectopic expression of neural autoantigen in mouse liver suppresses experimental autoimmune neuroinflammation by inducing antigen-specific Tregs. J Clin Invest 2008;118:3403–3410.
[7] Davidson A, Diamond B. Autoimmune diseases. N Engl J Med 2001;345:340–350.
[8] Rosenblum MD, Gratz IK, Paw JS, Abbas AK. Treating human autoimmunity: current practice and future prospects. Sci Transl Med 2012;4:125sr1.
[9] Wing K, Sakaguchi S. Regulatory T cells exert checks and balances on self tolerance and autoimmunity. Nat Immunol 2010;11:7–13.
[10] Carambia A, Herkel J. CD4 T cells in hepatic immune tolerance. J Autoimmun 2010;34:23–28.
[11] Longhi MS, Liberal R, Holder B, Robson SC, Ma Y, Mieli-Vergani G, et al. Inhibition of interleukin-17 promotes differentiation of CD25$^-$ cells into stable T regulatory cells in patients with autoimmune hepatitis. Gastroenterology 2012;142:1526–1535.
[12] Lapierre P, Béland K, Yang R, Alvarez F. Adoptive transfer of ex vivo expanded regulatory T cells in an autoimmune hepatitis murine model restores peripheral tolerance. Hepatology 2013;57:217–227.
[13] Leslie M. Immunology. Regulatory T cells get their chance to shine. Science 2011;332:1020–1021.
[14] Carambia A, Freund B, Schwinge D, Heine M, Laschtowitz A, Huber S, et al. TGF-β-dependent induction of CD4+CD25+Foxp3+ Tregs by liver sinusoidal endothelial cells. J Hepatol 2014;61:594–599.
[15] Petros RA, DeSimone JM. Strategies in the design of nanoparticles for therapeutic applications. Nat Rev Drug Discov 2010;9:615–627.
[16] Sørensen KK, McCourt P, Berg T, Crossley C, Le Couteur D, Wake K, et al. The scavenger endothelial cell: a new player in homeostasis and immunity. Am J Physiol Regul Integr Comp Physiol 2012;303:R1217–R1230.
[17] Baxter AG. The origin and application of experimental autoimmune encephalomyelitis. Nat Rev Immunol 2007;7:904–912.
[18] Liu GY, Fairchild PJ, Smith RM, Prowle JR, Kioussis D, Wraith DC. Low avidity recognition of self-antigen by T cells permits escape from central tolerance. Immunity 1995;3:407–415.
[19] Korn T, Reddy J, Gao W, Bettelli E, Awasthi A, Petersen TR, et al. Myelin-specific regulatory T cells accumulate in the CNS but fail to control autoimmune inflammation. Nat Med 2007;13:423–431.
[20] Huber S, Schramm C, Lehr HA, Mann A, Schmitt S, Becker C, et al. Cutting edge: TGF-beta signaling is required for the in vivo expansion and immunosuppressive capacity of regulatory CD4+CD25+ T cells. J Immunol 2004;173:6526–6531.
[21] Huber S, Stahl FR, Schrader J, Lüth S, Presser K, Carambia A, et al. Activin a promotes the TGF-beta-induced conversion of CD4+CD25− T cells into Foxp3+ induced regulatory T cells. J Immunol 2009;182:4633–4640.
[22] Freund B, Tromsdorf UI, Bruns OT, Heine M, Giemsa A, Bartelt A, et al. A simple and widely applicable method to 59Fe-radiolabel monodisperse superparamagnetic iron oxide nanoparticles [SPIOs] for in vivo quantification studies. ACS Nano 2012;6:7318–7325.
[23] Yu WW, Falkner JC, Yavuz CT, Colvin VL. Synthesis of monodisperse iron oxide nanocrystals by thermal decomposition of iron carboxylate salts. Chem Commun 2004;20:2306–2307.
[24] Li JJ, Wang YA, Guo W, Keay JC, Mishima TD, Johnson MB, et al. Large-scale synthesis of nearly monodisperse CdSe/CdS Core/Shell nanocrystals using air-stable reagents via successive ion layer adsorption and reaction. J Am Chem Soc 2003;125:12567–12575.
[25] Shtykova EV, Huang X, Gao X, Dyke JC, Schmucker AL, Dragnea B, et al. Hydrophilic monodisperse magnetic nanoparticles protected by an amphiphilic alternating copolymer. J Phys Chem C 2008;112:16809–16817.
[26] Sperling RA, Pellegrino T, Li JK, Chang WH, Parak WJ. Electrophoretic separation of nanoparticles with a discrete number of functional groups. Adv Funct Mater 2006;16:943–946.
[27] Braunsfurth JS, Gabbe EE, Heinrich HC. Performance parameters of the Hamburg 4 pi whole body radioactivity detector. Phys Med Biol 1977;22:1–17.
[28] Bruns OT, Ittrich H, Peldschus K, Kaul MG, Tromsdorf UI, Lauterwasser J, et al. Real-time magnetic resonance imaging and quantification of lipoprotein metabolism in vivo using nanocrystals. Nat Nanotechnol 2009;4:193–201.
[29] Bartelt A, Bruns OT, Reimer R, Hohenberg H, Ittrich H, Peldschus K, et al. Brown adipose tissue activity controls triglyceride clearance. Nat Med 2011;17:200–205.
[30] Pellegrino T, Manna L, Kudera S, Liedl T, Koktysh D, Rogach AL, et al. Hydrophobic nanocrystals coated with an amphiphilic polymer shell: a general route to water soluble nanocrystals. Nano Lett 2004;4:703–707.
[31] Bargheer D, Giemsa A, Freund B, Heine M, Waurisch C, Stachowski GM, et al. The distribution and degradation of radiolabelled SPIOs and Quantum Dots in mice. Beilstein J Nanotechnol 2015;6:111–123.
[32] Shimizu J, Yamazaki S, Sakaguchi S. Induction of tumor immunity by removing CD25+CD4+ T cells: a common basis between tumor immunity and autoimmunity. J Immunol 1999;163:5211–5218.
[33] Davidson TS, Shevach EM. Polyclonal Treg cells modulate T effector cell trafficking. Eur J Immunol 2011;41:2862–2870.
[34] Yeste A, Nadeau M, Burns EJ, Weiner HL, Quintana FJ. Nanoparticle-mediated codelivery of myelin antigen and a tolerogenic small molecule suppresses experimental autoimmune encephalomyelitis. Proc Natl Acad Sci U S A 2012;109:11270–11275.
[35] Getts DR, Martin AJ, McCarthy DP, Terry RL, Hunter ZN, Yap WT, et al. Microparticles bearing encephalitogenic peptides induce T-cell tolerance and ameliorate experimental autoimmune encephalomyelitis. Nat Biotechnol 2012;30:1217–1224.
[36] Palucka K, Banchereau J, Mellman I. Designing vaccines based on biology of human dendritic cell subsets. Immunity 2010;33:464–478.
[37] Sica A, Mantovani A. Macrophage plasticity and polarization: in vivo veritas. J Clin Invest 2012;122:787–795.
[38] Kern M, Popov A, Scholz K, Schumak B, Djandji D, Limmer A, et al. Virally infected mouse liver endothelial cells trigger CD8+ T-cell immunity. Gastroenterology 2010;138:336–346.
[39] Klugewitz K, Blumenthal-Barby F, Schrage A, Knolle PA, Hamann A, Crispe IN. Immunomodulatory effects of the liver: deletion of activated CD4+ effector cells and suppression of IFN-gamma-producing cells after intravenous protein immunisation. J Immunol 2002;169:2407–2413.

[40] Kruse N, Neumann K, Schrage A, Derkow K, Schott E, Erben U, et al. Priming of CD4+ T cells by liver sinusoidal endothelial cells induces CD25low forkhead box protein 3-regulatory T cells suppressing autoimmune hepatitis. Hepatology 2009;50:1904–1913.
[41] Yadav M, Stephan S, Bluestone JA. Peripherally induced Tregs – Role in immune homeostasis and autoimmunity. Front Immunol 2013;4:232.
[42] Schurich A, Böttcher JP, Burgdorf S, Penzler P, Hegenbarth S, Kern M, et al. Distinct kinetics and dynamics of cross-presentation in liver sinusoidal endothelial cells compared to dendritic cells. Hepatology 2009;50:909–919.